on an empirical formula relating them to the effective stress and hence, to the level of mechanical compaction.

Here empirical relation q=0.36+0.98p has been adopted. Schematic diagram for the rock physics template for Soft Sand Model 1 and 2 is shown in Fig.2.

Dry rock frame obtained either from Soft Sand Model 1(Eqn.3) or Soft sand Model 2 (Eqn.6) including fluid moduli (Eqn.2) when put in Gassmann's equation (Eqn.1) results in elastic properties (Vp, Vs or *Mb*) of the target reservoirs for different fluid scenarios. Bulk density is obtained from

$$\rho b = \rho m\,(1 - \phi) + \rho f\,\phi \qquad (7)$$

where ρm and ρf are matrix and fluid density respectively. The elastic properties are plotted on a template containing acoustic impedance (AI) vs. reservoir property (ϕ) to understand the impedance contrasts for sand-shale combinations assuming different fluid scenarios.

Notice that in Gassmann fluid substitution, isotropic medium has been assumed. Isotropic fluid operations are fairly accurate in case of weak anisotropy produced by weak elastic contrasts (Mavko and Bandyopadhyay, 2008).

For rock physics modeling, Vcl (smectite)=10% and Vqtz=90% has been assumed because sand intervals under study has Vcl range ~10-15%.The rock physics models-Soft sand Model 1 (at 10, 20 and 30 MPa) and Soft Sand Model 2 have been generated considering minerals such as quartz and clay by corroborating with drill cuttings in the intervals of interests with their fractions 90% quartz and 10% clay for cleaner sands.

Soft Sand Model 1 at 10, 20 and 30 MPa is realized using three end member pairs of ϕcon and ϕc: 18-30%, 22 to 34%, and 26 to 38%.Four curves of Soft Sand Model 2, representing pore-shape factors p of 15, 25, and 45, cross the grain of model 1 at oblique angles (Fig.3).Other material properties considered in modeling has been shown in Table-1.

Discussions

Each pay interval whether saturated with oil (e.g. S1 of well 1) or gas (S3 of Well 2) produce seismic anomaly whereas water saturated sands (S1 of Well 2) has feeble amplitudes as shown in Fig.1a and 1b. The dry frames of the pay sands (obtained from rearranging the Gassmann's equation) encountered in Well 1 and 2, when plotted with porosity, appear to be softer (i.e. lower pore space stiffness) and congressional modulus increases slightly in gradual fashion with the decrease in porosity along Soft Sand Model 2 at pore shape factor P3:45 (Fig.3).

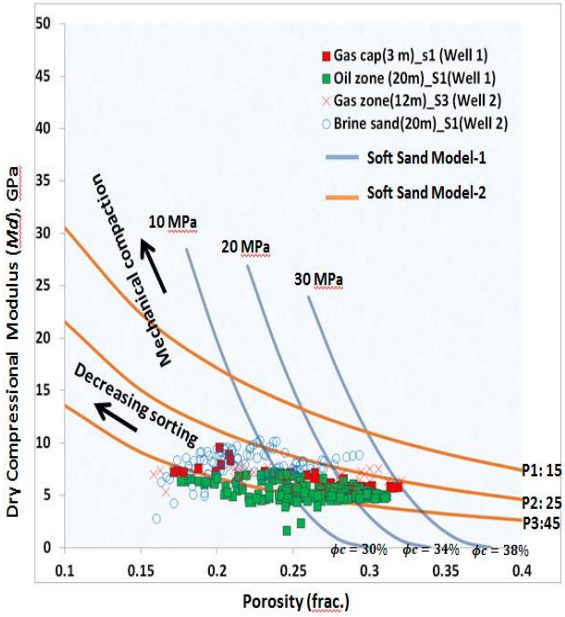

Fig.3 Rock physics template showing Soft Sand Model 1 and 2 with inverted dry compressional modulus (inverted from logs) of the sands under study. The dry frame sand intervals from logs are color coded just to know whether it is from oil or gas zones.

Pore shape is dominantly a function effective stress along mechanical compaction trend and it decreases with increase in the effective pressure i.e p=A.σ^{-B}, where σ is effective stress (Mpa) and the parameters A and B are affected by the level of elastic unloading that is due to overpressure or uplift or erosion late in diagenetic history (Vernik, L., pg. 64, 2016). Here σ=25MPa, A=700 and B=0.85 have been considered. Apart from P3 at 45, two other Soft Sand Model lines were generated at P1:15 and 25 to assess the impact

of the effective stress at both the locations. This suggests that the dry frames of the pay sands from both the locations plot majorly along a single modeled line. The template exhibits that even at ~18% porosity, the compaction trend is not changing; this suggests that the sands are soft and un-cemented.

Further, the sands are deposited in deltaic environment and petrophysical analysis (not covered in this paper) suggests that salinity of the sands is in the range of 34000-36000 ppm. The average effective pressure of the reservoirs from the locations is 25 MPa. This suggests that effects of sediment compaction and salinity of brine are almost similar at the locations.

The area of study also does not have any history of thin or thick skin tectonic inversion. Therefore, tectonic inversion related rock fracturing can be ruled out.

Moreover, as far as source rock and its type (Type II and III in our case) is concerned, it is either below the intervals of study or basinward on the basis of regional data study. As we know thermally matured and organically rich source rock when overlain by inorganic shale generate seismic anomaly. This also suggests that the intervals of study are also not affected by source rock.

Temperature range of the reservoirs is 50-60 deg. Cel. When the in-situ temperature ranges from 70 to 150 Deg. Cel. smectite alters to illite (Bruce, 1984; Swarbrick and Osborne, 1998) and this process leads to the grain contacts getting cemented because of quartz precipitation. This also suggests that the reservoir intervals S1, S2 and S3 don't have enough temperature to initiate chemical compaction because the clay mineral has not undergone transformation due to lower temperature than required (e.g. smectite to illite).Nonetheless, it has assumed here the lowest consolidation porosity ϕcon is 18% for soft Sand Model 1 and below this porosity, chemical consolidation may begin owing to temperature driven mineral transformation. Further, Fig.3 also infers that the critical porosity ϕc (i.e. depositional porosity) in the intervals are varying from 38 to 30% and is further less depending upon sorting, which ultimately is linked to environment of deposition. The template in Fig.3 does show data points to the left of Soft sand Model 1(10 Mpa) which indicates that sorting is further poorer. None of the pay intervals show dominant trend along Soft Sand Model 1. Therefore, Rock physics template suggests that the reduction in porosity and gradual increase in velocity is due to sorting effect under similar effective pressure from both the locations.

Fluid effect on the seismic amplitude depends upon the stiffness of the frame. In this case study, the pay sands appear to be unconsolidated and un-cemented. The pore saturating fluids are oil (40 deg. API) and gas. This suggests that the sensitivity of the seismic amplitudes to the fluid is expected.

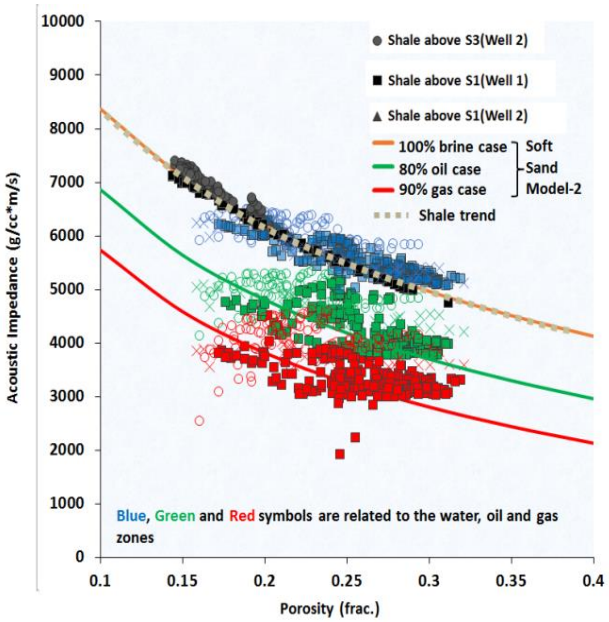

Fig.4 showing the soft sands in different fluid scenarios (oil, gas and water) and the shales from the top of the respective sands. Impedance contrasts between shales and water sands are feeble whereas hydrocarbon saturated sands are well separated.

Under the in-situ conditions, the pay sands are saturated with different fluids (i.e. oil, gas). After Gassmann's fluid substitution, the sands are taken to a common fluid level i.e. 100 % brine saturation, then replaced with oil (So=80%) and gas (Sg=90%) and have been shown in acoustic impedance vs. porosity plane (Fig. 4). Shales are also plotted by selecting from the top of the respective sand intervals. Fig.4 shows that the impedance contrast between shales and the water sands are not

significant .This means the expectations in terms of seismic amplitude from the shale/water sand interface are feeble across the porosity range ~18-33%. The oil saturated sands fall almost in the middle of gas sands and shales. This shows that oil zones can also be detected besides gas under this type of geological set up.

Conclusions

Rock physics analysis suggests that sands in the study area are un-consolidated and un-cemented. The dominant geological factors extracted from the compressional modulus-porosity plane after establishing relationship between elastic and reservoir property & lithology are sorting of the sands and the type of the fluid present in it. Therefore, the seismic amplitudes are controlled by sorting and fluid effect rather than the other competing geological factors, as supported by the seismic amplitudes at the drilled locations. Rock physics template also assess that the pore spaces are of concave geometry. Shales and water sand combinations are found to generate feeble amplitude. Other seismic phenomenon, that is tuning effect, which is not discussed in this paper, can also affect the amplitudes.

Acknowledgement

Authors are thankful to the organization, Essar Exploration and Production Ltd.(EEPL) for allowing to publish this paper.

References

Bruce, C. H., 1984, Smectite dehydration: Its relation to structural development and hydrocarbon accumulation in northern Gulf of Mexico Basin: AAPG Bulletin, 68, 673–683.

Biot, M., 1956, Theory of propagation of elastic waves in a fluid-saturated porous solid. Low-Frequency Range, The journal of the acoustic society of America, Vol. 28, No. 2, 168-178.

Dunne, J. 2011, Geologic controls on seismic amplitudes, ResearchGate.

Dvorkin, J., Gutierrez, M., Grana, D., 2014, Seismic reflections of rock properties, Cambridge University Press

Gassmann, F. (1951). Elasticity of porous media: Uber die elastizitat poroser medien: ierteljahrsschrift der Naturforschenden, Gesselschaft, 96, 1–23.

Mavko, G., and K. Bandyopadhyay, 2009, Approximate fluid substitution for vertical velocities in weakly anisotropic VTI rocks: Geophysics, 74, no. 1, D1–D6, doi: 10.1190/1.3026552.

Swarbrick, R. E., and M. J. Osborne, 1998, Mechanisms that generate abnormal pressures: An overview, in G. F. Ulmishek and V. I. Slavin, eds., Abnormal pressure in hydrocarbon environments: AAPG Memoir 70, 13–34.

Vernik, L., 1998, Acoustic velocity and porosity systematics in siliciclastics: The Log Analyst, 39, 27–35.

Vernik, L., and M. Kachanov, 2010, Modeling elastic properties of siliciclastic rocks: Geophysics, 75, no. 6, E171–E182, http://dx.doi.org/10.1190/1.3494031

Vernik, L., 2016, Seismic Petrophysics in Quantitative Interpretation, Society of Exploration Geophysicists.

Table-1

Material properties used in the modeling	
Km qtz	36.6 GPa
Gm qtz	45 GPa
Km cl	21 GPa
Gm cl	7 Gpa
Koil	0.792 GPa
Kgas	0.036 GPa
Kbrine	2.69 GPa
ρ qtz	2.65 g/cc
ρ clay	2.2 g/cc
ρ brine	1.018 g/cc
ρ oil	0.622 g/cc
ρ gas	0.182 g/cc
GOR	176 l/l
Salinity	36000 ppm
Reservoir Pressure	24 MPa
Overburden	49 MPa
Effective Pressure	25 MPa
Temp.	60 deg Cel
Oil API	40 Deg.